

# Optically scanned laser line sensor

Johannes Schlarp, Ernst Csencsics and Georg Schitter, *Senior Member, IEEE*,  
 Christian Doppler Laboratory for Precision Engineering for Automated In-Line Metrology  
 Automation and Control Institute (ACIN), Technische Universität Wien  
 Vienna, Austria  
 schlarp@acin.tuwien.ac.at

**Abstract**—This work presents the system design, motion control and the evaluation of an optical scanning system, which manipulates only the illumination path of a laser line sensor by a galvanometer scanner. The selected system design minimizes aberrations due to the optical scanning through the scanner placement. The surface profile is reconstructed from the measured quantities and the model parameters using geometrical relations. An adapted triangular scan trajectory, which features a constant scan speed, is used to scan the sample, such that a uniform lateral resolution is achieved. To follow the scan trajectory a PID feedback controller with a closed loop bandwidth of 305 Hz is designed. The field of view of 31x36 mm is obtained with a resolution of 300x400 pixels. The scanning system achieves a framerate of up to 0.67 frames/s. Experimental results show that the achievable resolution is comparable to the one of a classical mechanical scanning system.

**Index Terms**—Optical sensors, Precision engineering, Sensor Systems, Metrology, Optical devices, Linear feedback control systems

## I. INTRODUCTION

In the manufacturing industry the demands for precise and fast measurement systems are constantly growing [1]. For in-line metrology the measurement system should be able to capture not only one specific dimension on the sample but rather the entire sample, such that the amount of measurement procedures and the overall measurement time can be reduced [2]. Typical applications of three dimensional (3D) measurement systems are the inspection of weld seams [3], the verification of the dimensional accuracy of machined components, e.g. injection moulded parts [4], and the inspection of the position and orientation of several parts in an assembly, e.g. circuit board assembly [5]. State of the art 3D measurement systems, which are already integrated into manufacturing lines are mostly camera based systems, like fringe projection systems [6], [7]. The resolution of these optical sensor systems is, however, limited to a few micrometre [8].

If a higher resolution is required, generally mechanical scanning systems, e.g. coordinate measurement machines (CMM), are used [9]. These systems use external actuators to position a tactile probe over the sample, which triggers if the probe is in contact with the sample [10]. To improve the measurement speed of CMM's and avoid the contact between sensor and sample during the measurement, which could impair the sample, optical sensors are used instead of the tactile probe [11]. Due to the large moving mass the achievable scan speed of these systems is, however, strongly limited [12].

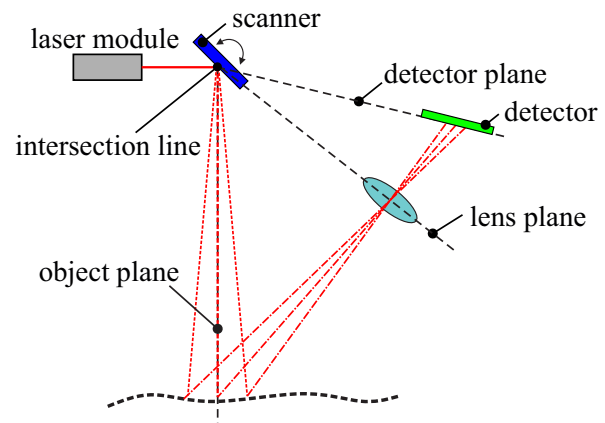


Fig. 1. Schematic of an optical scanning system, which satisfies the Scheimpflug condition.

In [13] an optical scanning system is presented, which manipulates the optical path of a laser triangulation sensor by means of a fast steering mirror. An optical scanning system can achieve a higher scan speed as compared to a classical mechanical scanning system, due to the lower moving mass. The optical design of the scanning system is further improved in [15], such that the Scheimpflug condition, which is a generalized form of the thin lens equation for non parallel planes [16], is satisfied by the system even though only the illumination path is manipulated by a fast steering mirror. This is realized by placing the scanner on the intersection line of the object, lens and detector plane, which is shown in Fig. 1. However, the scanning system uses a dot laser module, such that only a single point is scanned at a time. Laser triangulation sensors are available as point sensors, but also as laser line sensors, such that an optical scanning system with an even higher scan speed can be realized.

The contribution of this paper is the system design, surface reconstruction, control and evaluation of an optical scanning laser line sensor. Section II describes the system design, the geometrical relations, which are used to reconstruct the surface of the sample from the measured quantities and the experimental setup. Possible scan trajectories are discussed in Section III, followed by the system identification and controller design shown in Section IV. The measurement results are presented in Section V and Section VI concludes the paper.

## II. SYSTEM DESCRIPTION

### A. System Design

The system design is based on a commercial laser line sensor (Type: LLT 2660-50, Micro-Epsilon GmbH, Germany) with a measurement range of 50 mm in the  $x$  and  $z$ -direction and a resolution of 640 points/profile for the  $x$ -direction and  $4 \mu\text{m}$  in the  $z$ -direction. The laser line sensor provides a two dimensional measurement, such that the position of the laser line needs to be changed only in one direction to generate a three dimensional image. This is realized by redirecting the optical path of the laser line by means of an galvanometer scanner (Type: 6870M, Cambridge Technology, USA). This actuator type is applied in various scanning systems, like stereo lithography [17], lidar systems [18] and laser machining [19]. The main components of a galvanometer scanner are a coil, which actuates a magnet with an attached optical mirror. The moving part is guided by a set of bearings and the angular position is measured by an internal sensor system.

The mirror surface of the galvanometer scanner is placed on the intersection line of the object, lens and detector plane, such that aberrations due to the optical scanning are minimized [15]. The position of the intersection line can be derived from the position and orientation of the lens and detector plane, which are fixed by the laser line sensor. The lens and detector plane intersect within the housing of the laser line sensor, such that the scanner can not be placed directly on the intersection line. Therefore, the internal laser line module of the sensor is disconnected, instead the sample is illuminated by an external laser line module with an equal wavelength (658 nm).

By inserting an additional static mirror in the illumination path, the optical path can be folded, such that the scanner is optically positioned on the intersection line. Therefore, the distance  $d_{Galvo}$  between the scanner and the static mirror should be equal to the distance between the static mirror

and the intersection line. The size of the static mirror is determined in one direction by the distance  $d_{Galvo}$  and the actuation range of the scanner ( $\pm 4^\circ$ ), and in the other direction by the distance  $d_{Galvo}$  and the fan angle of the laser line module ( $25^\circ$ ). A squared static mirror with dimensions of  $50.8 \times 50.8 \text{ mm}$  (BBSQ2-E02, Thorlabs Inc., USA) is used to deflect the laser line. For an easy and precise alignment of the optical components the static mirror and galvanometer scanner are rotated by  $45^\circ$  with respect to the  $xy$ -plane.

### B. Geometrical relations for surface reconstruction

The measured quantities are the angular position  $\varphi$  of the galvanometer scanner and the measured profile described by  $x_{meas}$  and  $z_{meas}$ . The surface profile of the sample is described by the absolute quantities  $x_s$ ,  $y_s$  and  $z_s$ . In order to reconstruct the surface profile out of the measured quantities, the geometrical relations need to be determined up front. Therefore, the similarity theorem for triangles and trigonometry are used [20]. With the triangles, depicted in Fig. 3 (dashed yellow and dashed green), the relation between the measured distance  $z_{meas}$  and the absolute distance  $z_s$  can be formulated as

$$\frac{z_{meas} + z_{lens}}{y_{lens}} = \frac{z_s + z_{lens}}{y_{lens} + y_s}, \quad (1)$$

in which  $y_{lens}$  and  $z_{lens}$  describe the position of the lens in the  $y$  and  $z$ -direction, respectively. The exact position of  $y_{lens}$  and  $z_{lens}$  were provided by the manufacturer of the laser line sensor. This positions are referred to the exit point of the laser line from the sensor, which is selected as the point of origin. The value of  $y_s$  can be calculated with trigonometry to

$$\tan(2\varphi) = \frac{y_s}{z_s + z_{galvo}}, \quad (2)$$

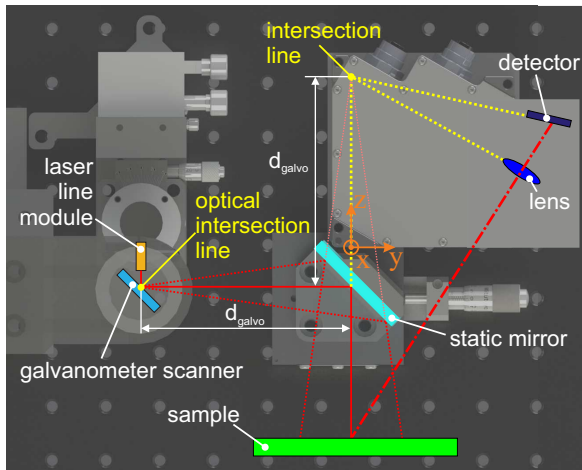


Fig. 2. System design of the scanning laser line system. The position of the laser line on the sample is varied by a galvanometer scanner.

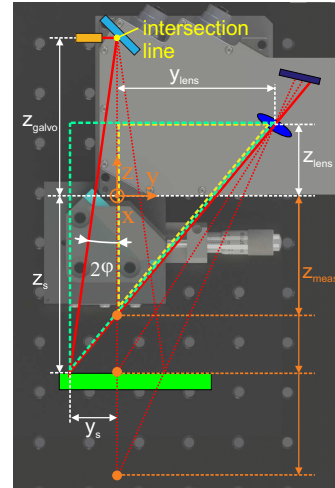


Fig. 3. Characteristic dimensions of the system. The similarity of triangles is used to reconstruct the surface profile of the sample.

with the measured angular position  $\varphi$  and the distance  $z_{galvo}$  between the intersection line and the point of origin. Since the profile is measured along the  $z$ -axis, the absolute value  $x_s$  has to be calculated with the similarity of triangles as follows

$$\frac{z_{meas} + z_{galvo}}{x_{meas}} = \frac{z_s + z_{galvo}}{x_s}. \quad (3)$$

By rearranging Eqn. (1)-(3) the 3D surface profile of the sample can be calculated by

$$z_s = \frac{z_{meas} y_{lens} + z_{galvo} \tan(2\varphi)(z_{meas} + z_{lens})}{y_{lens} - \tan(2\varphi)(z_{meas} + z_{lens})} \quad (4a)$$

$$y_s = (z_s + z_{galvo}) \tan(2\varphi) \quad (4b)$$

$$x_s = x_{meas} \frac{z_s + z_{galvo}}{z_{meas} + z_{galvo}}. \quad (4c)$$

### C. Experimental Setup

Figure 4 shows the experimental setup. As can be observed, the various components are mounted on manual linear and rotational stages, to align them with respect to each other. To control the galvanometer scanner a rapid prototyping system (Type: DS1202, dSPACE GmbH, Germany) with a sampling rate of 40 kHz is used. The measurement of the laser line sensor is triggered by the dSpace platform, such that the measured profile is synchronized with the position of the galvanometer scanner. After the sample is scanned the data of the laser line sensor are transferred and merged with the measured angular position of the galvanometer scanner, such that the surface profile can be reconstructed. As can be observed in Fig. 4, the sample is mounted on a position controlled stage (Type: VT-80, Physik Instrumente, Germany), such that also reference measurements can be performed. The motorized stage features an actuation range of 200 mm with a resolution of 500 nm.

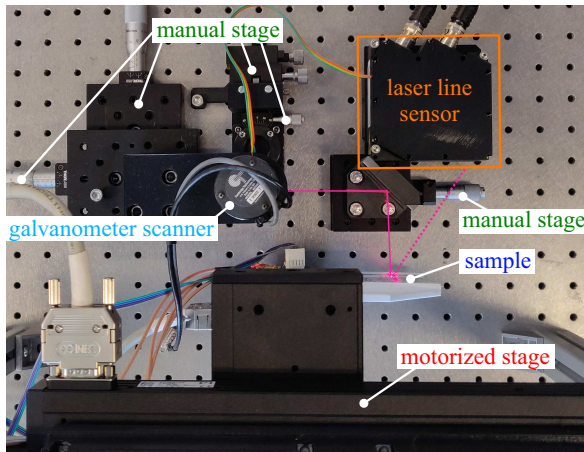


Fig. 4. Experimental setup of the scanning laser line sensor.

### III. SCAN TRAJECTORY

To scan the area of interest on the sample with the galvanometer scanner, an appropriate scan trajectory is required. Triangular scan patterns are frequently used in optical scanning systems, due to their uniform scan speed [21]. The scan frequency depends on the selected resolution and profile rate of the laser line sensor, such that a trade-off between the lateral scan range and measurement speed has to be made. The resolution of the optical scanning system is selected to 300 pixel along the scan direction and 400 pixel for the laser line sensor, which enables to capture 400 profiles/s. Only the rising half of the triangular signal is used to scan the sample, such that the frequency needs to be 600 times lower as compared to the profile rate. With the selected frequency  $f_{tr}$  of 0.375 Hz, a framerate of 0.67 frames/s can be achieved. For an actuation range of  $\pm 4^\circ$  the achievable scan range in the  $y$ -direction is 36 mm, while the scan range in the  $x$ -direction is 31 mm at a distance  $z_s$  of 95 mm. The achievable resolution of the scanning system in the  $x$  and  $z$ -direction is mainly determined by the triangulation sensor, which is  $77.5 \mu\text{m}$  and  $4 \mu\text{m}$ , respectively. The resolution in the  $y$ -direction is determined by the angular resolution of galvanometer scanner, which is 2.25 mdeg. This resolution can be calculated with Eqn. 4 to  $14 \mu\text{m}$ .

The triangular scan trajectory generates a uniform angular scan speed for the angle  $\varphi$ . The lateral scan speed over the sample is, however, non uniform (see Fig. 5), due to the non-linear relation between  $\varphi$  and  $y_s$  in Eqn. (2). The time dependency of the angle  $\varphi$  for the triangular signal can be

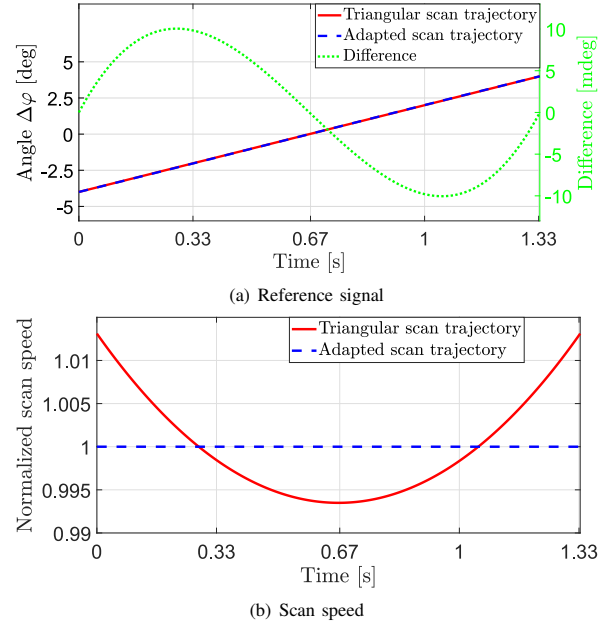


Fig. 5. Scan trajectories and corresponding scan speeds of the galvanometer scanner.

described with

$$\varphi(t) = \frac{(\varphi_{max} - \varphi_{min})f_{tr}}{2}t + \varphi_{min}, \quad (5)$$

in which  $\varphi_{max}$ ,  $\varphi_{min}$  describe the maximum and minimum angular position of the galvanometer scanner. By adapting the triangular scan trajectory to

$$\varphi_d(t) = \tan^{-1} \left[ \frac{(\varphi_{max} - \varphi_{min})f_{tr}}{2}t + \varphi_{min} \right], \quad (6)$$

a constant lateral scan speed over the sample can be achieved, such that an image with a uniform lateral resolution is generated. Figure 5 shows the two scan trajectories, the difference between them, and the normalized scan speed over the sample.

#### IV. MOTION SYSTEM

##### A. System Identification

The motion controller is an essential part of the overall scanning system, since it determines how accurate the galvanometer scanner tracks the scan trajectory [22]. A good tracking performance ensures that the selected lateral resolution is maintained. In order to design a tailored feedback controller for the galvanometer scanner, an exact mechanical model of the scanner is necessary. To obtain this model the frequency response is measured with a system analyzer (Type: 3562A, Hewlett-Packard, USA). The current through the coil of the galvanometer scanner and the angular position  $\varphi$  are considered as the system input and output, respectively.

The measured frequency response data (solid red) are shown in Fig. 6. The strongly damped suspension mode of the scanner lies at 42 Hz and the first structural mode of the scanner is at 5.75 kHz. The noise floor of the system ( $\sim -60$  dB) is reached at about 2 kHz. At frequencies below 30 Hz an additional phase lag is observable, which is caused by the non-linear dynamics of the bearing friction [23].

To model the system dynamics a fourth-order transfer function (TF) with a time delay is used

$$G(s) = \frac{K\omega_0^2}{s^2 + 2\zeta_0\omega_0 + \omega_0^2} \cdot \frac{s^2 + 2\zeta_1\omega_1 + \omega_1^2}{s^2 + 2\zeta_2\omega_2 + \omega_2^2} \cdot e^{-sT_a}, \quad (7)$$

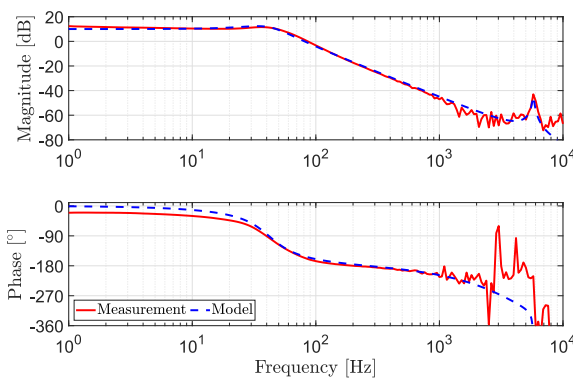


Fig. 6. Measured and modelled frequency response of the galvanometer scanner.

with the DC gain  $K=3.16$  and the parameters according to Table I. The time delay of  $T_a=100 \mu s$  is used to model the phase lag of the dSpace platform (40 kHz) and the position sensor of the galvanometer scanner. The modelled TF (dashed blue) depicted in Fig. 6, shows a good agreement with the measurement.

TABLE I  
COEFFICIENTS OF THE SYSTEM MODEL.

Index	$\omega_{Index}$ [rad/s]	$\zeta_{Index}$
0	263.88	0.42
1	3.62e4	0.5
2	3.62e4	0.015

##### B. Motion Control

The design of the position controller  $C(s)$  for the galvanometer scanner is done with the aim to follow the triangular scan trajectory and to suppress external disturbances [22]. Based on the derived system model, a feedback controller is designed with the PID alpha tuning method for a crossover frequency of 200 Hz. The selected crossover frequency is sufficient to suppress the influence of the bearing friction, which is described in Chapter IV-A, on the closed loop operation [24]. With the alpha tuning method the trade-off between performance and robustness of the PID feedback controller can be adjusted with just one parameter the  $\alpha$ -value [25]. Since the optical scanning system should be robust against external disturbances, which could change the system dynamics of the galvanometer scanner a  $\alpha$ -value of 3.5 is selected. To suppress the first structural mode, an additional notch filter is applied at 5.7 kHz, such that the controller has the following form

$$C(s) = K_C \frac{\prod_{i=0}^1 s^2 + 2\zeta_{zi}\omega_{zi} + \omega_{zi}^2}{\prod_{j=0}^1 s^2 + 2\zeta_{pj}\omega_{pj} + \omega_{pj}^2} \quad (8)$$

with the gain  $K_C=26.7975$  and the parameters according to Table II. Figure 7 depicts the TF of the controller (dash-dotted

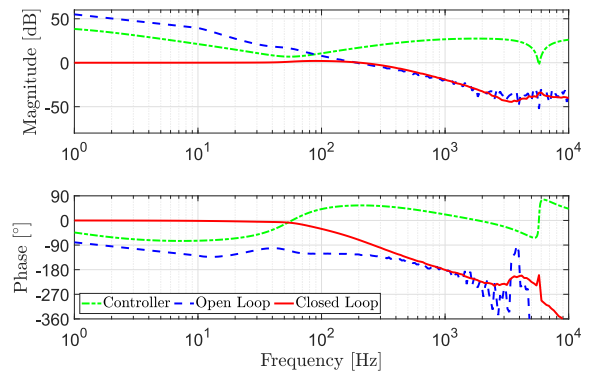


Fig. 7. Modelled controller TF, measured loop gain and complementary sensitivity function of the galvanometer scanner.

green). It is observable that the controller features a high gain for low frequencies, which leads to a zero steady state error. At the crossover frequency the phase of the controller reaches the maximum of  $55^\circ$ , such that a sufficient phase margin is achieved. Figure 7 also shows the measured open loop frequency response (dashed blue). The phase margin of  $55.6^\circ$  can be observed at the crossover frequency (195 Hz), the gain margin of the system is 16.9 dB. The measured complementary sensitivity function (solid red) is also shown in Fig. 7. As can be observed, the maximum gain peaking of the system is 2 dB, while the -3 dB bandwidth is reached at 305 Hz.

TABLE II  
COEFFICIENTS OF THE MOTION CONTROLLER.

Index	$\omega_{zIndex}$ [rad/s]	$\zeta_{zIndex}$	$\omega_{pIndex}$ [rad/s]	$\zeta_{pIndex}$
0	348.22	0.52	166.24	13.25
1	3.62e4	0.015	3.62e4	0.5

## V. EVALUATION OF THE SYSTEM PERFORMANCE

To validate, if the optical scan influences the achievable system performance, a measurement on a resolution test target is performed (Type: R3L3S1P, Thorlabs, USA), which conforms to the MIL-S-150A standard. The measurement result is compared against a reference measurement obtained with the mechanical scanning system, described in Section II-C. The sample features a line pattern with a defined width and

spacing, which has a tolerance of  $\pm 0.5 \mu\text{m}$  and  $\pm 1 \mu\text{m}$ , respectively. The first element of the group -2 is measured, which has a line width of 2 mm for the parameters  $\Delta x$  and  $\Delta y$ . Figure 8 depicts the sample, the selected feature and the measurement result of the optical scan, which shows a good agreement with the shown result of the mechanical scan. In the optical scan a degradation of the horizontal features towards the edge ( $y=12 \text{ mm}$ ) is observable. This error is caused by a defocus of the projected laser line on the detector. The laser line sensor uses a lens with a fixed focal length, such that a rotation of the object plane around the intersection line (see Fig. 1) leads to a rotation of the detector plane. The error could be partially corrected by taking the defocus into account for the surface reconstruction. The calculated dimension and standard deviation of  $\Delta x$  and  $\Delta y$  for the optical and mechanical scan are summarized in Table III. For the optical scan the measured dimension  $\Delta x$  is lower compared to the mechanical scan, which is caused by the defocus. Furthermore, this causes a larger standard deviation for the optical scan. This is also observable in Fig. 9, which shows the distribution of the measured line widths for both scanning system. The measured dimension along the scan axis is limited by the selected resolution of  $100 \mu\text{m}$ , such that the deviation from the defined line width (2 mm) is within the resolution. The dimension  $\Delta y$  of the optical scan matches the one of the mechanical scan (see Fig. 9), such that the achievable resolution in the  $y$ -direction is not impaired by the optical scan.

In summary, the feasibility of an optical scanning line sensor system, which manipulates only the illumination path with a galvanometer scanner is demonstrated, achieving a measurement range of  $31 \times 36 \times 50 \text{ mm}$  and a framerate of up to 0.67 frames per second.

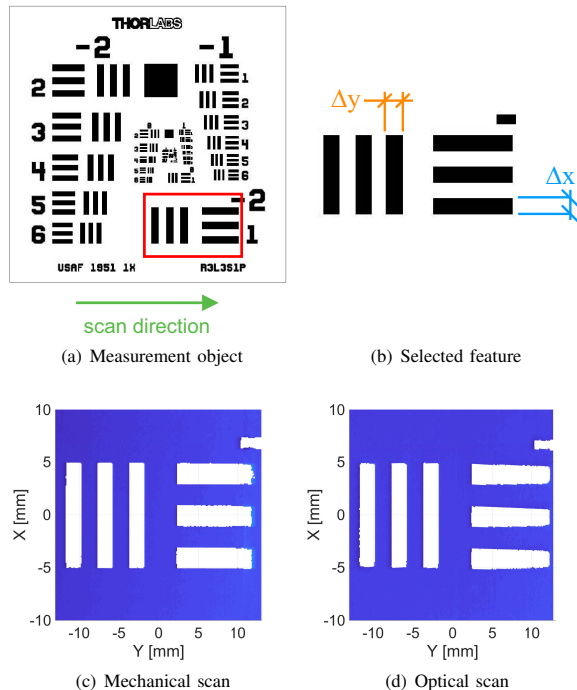


Fig. 8. Measurement object and measurement results of the optical and mechanical scanning systems.

TABLE III  
MEASURED LINE WIDTH.

Dimension	Mechanical scan		Optical scan	
	Mean value	Std. deviation	Mean value	Std. deviation
$\Delta x$	1.958 mm	33.9 $\mu\text{m}$	1.836 mm	87.7 $\mu\text{m}$
$\Delta y$	1.9 mm	0 $\mu\text{m}$	1.937 mm	0.5 $\mu\text{m}$

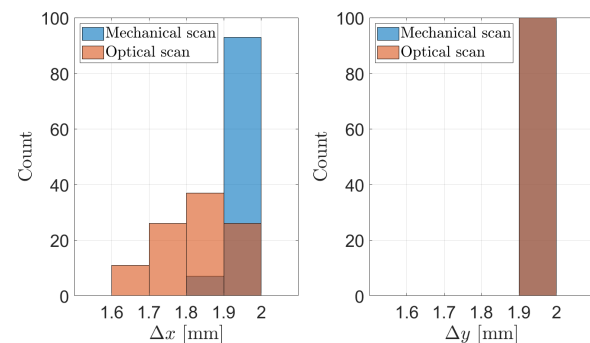


Fig. 9. Distribution of the measured line width  $\Delta x$  and  $\Delta y$ .

## VI. CONCLUSION

This paper presents the design, control and the measurement results of an optical scanning line sensor system, which manipulates only the illumination path with a galvanometer scanner. By placing the scanner on the intersection line, aberrations due to the optical scanning can be minimized. With the geometrical relations, which are determined from the system design, the surface of the sample can be reconstructed from the measured quantities. To scan the area of interest adapted triangular scan trajectories are employed, such that a uniform lateral resolution is obtained. To track the scan trajectory, a PID feedback controller is designed. The controller design is based on the identified system dynamics and achieves a closed loop bandwidth of 305 Hz. The measurement result of the optical scan matches with the result of a mechanical scanning system and the defined dimensions of the sample. Therefore, it can be concluded that fast and precise 3D measurements with an optical scanning line sensor system are feasible. Future research work is concerned with the correction of the defocus, such that the achievable resolution can be further improved.

## ACKNOWLEDGMENT

The financial support by the Christian Doppler Research, the Austrian Federal Ministry for Digital and Economic Affairs and the National Foundation for Research, Technology and Development, as well as MICRO-EPSILON MESSTECHNIK GmbH & Co. KG and ATENSOR Engineering and Technology Systems GmbH is gratefully acknowledged.

## REFERENCES

- [1] H. Schwenke, U. Neuschaefer-Rube, T. Pfeifer, and H. Kunzmann, "Optical methods for dimensional metrology in production engineering," *CIRP Annals-Manufacturing Technology*, vol. 51, no. 2, pp. 685–699, 2002.
- [2] R. Schmitt and F. Moenning, "Ensure success with inline-metrology," *XVIII IMEKO world congress Metrology for a Sustainable Development*, 2006.
- [3] Y. Li, Y. F. Li, Q. L. Wang, D. Xu, and M. Tan, "Measurement and defect detection of the weld bead based on online vision inspection," *IEEE Transactions on Instrumentation and Measurement*, vol. 59, no. 7, pp. 1841–1849, 2009.
- [4] C. P. Keferstein and W. Dutschke, *Fertigungsmesstechnik*. Wiesbaden: Springer Vieweg, 2010.
- [5] J. A. Jalkio, R. C. Kim, and S. K. Case, "Three dimensional inspection using multistribe structured light," *Optical Engineering*, vol. 24, no. 6, p. 246966, 1985.
- [6] G. Sansoni, M. Trebeschi, and F. Docchio, "State-of-the-art and applications of 3d imaging sensors in industry, cultural heritage, medicine, and criminal investigation," *Sensors*, vol. 9, no. 1, pp. 568–601, 2009.
- [7] T. Tao, Q. Chen, J. Da, S. Feng, Y. Hu, and C. Zuo, "Real-time 3-d shape measurement with composite phase-shifting fringes and multi-view system," *Optics express*, vol. 24, no. 18, pp. 20 253–20 269, 2016.
- [8] F. Blais, "Review of 20 years of range sensor development," *Journal of Electronic Imaging*, vol. 13, no. 1, 2004.
- [9] J. A. Sladek, *Coordinate Metrology*. Springer, 2016.
- [10] A. Weckenmann, T. Estler, G. Peggs, and D. McMurtry, "Probing systems in dimensional metrology," *CIRP Annals-Manufacturing Technology*, vol. 53, no. 2, pp. 657–684, 2004.
- [11] R. Leach, *Optical measurement of surface topography*. Berlin Heidelberg: Springer, 2011, vol. 14.
- [12] C. Yu, X. Chen, and J. Xi, "Modeling and calibration of a novel one-mirror galvanometric laser scanner," *Sensors*, vol. 17, no. 1, p. 164, 2017.
- [13] J. Schlarp, E. Csencsics, and G. Schitter, "Optical scanning of a laser triangulation sensor for 3d imaging," *IEEE Transactions on Instrumentation and Measurement*, 2019, accepted.
- [14] F. J. Brosed, J. J. Aguilar, D. Guilloma, and J. Santolaria, "3d geometrical inspection of complex geometry parts using a novel laser triangulation sensor and a robot," *Sensors*, vol. 11, no. 1, pp. 90–110, 2010.
- [15] J. Schlarp, E. Csencsics, and G. Schitter, "Scanning laser triangulation sensor geometry maintaining imaging condition," *Proceedings of the 8th IFAC Symposium on Mechatronic Systems*, pp. 301–306, 2019.
- [16] M. Bass, E. W. Van Stryland, D. R. Williams, and W. L. Wolfe, *Handbook of optics*. New York: McGraw-Hill, 2001, vol. 2.
- [17] I. Gibson, D. W. Rosen, B. Stucker et al., *Additive manufacturing technologies*. Springer, 2014, vol. 17.
- [18] F. Hosoi and K. Omasa, "Voxel-based 3-d modeling of individual trees for estimating leaf area density using high-resolution portable scanning lidar," *IEEE Transactions on Geoscience and Remote Sensing*, vol. 44, no. 12, pp. 3610–3618, 2006.
- [19] G. F. Marshall and G. E. Stutz, *Handbook of optical and laser scanning*. CRC Press, 2004.
- [20] O. Byer, F. Lazebnik, and D. L. Smeltzer, *Methods for Euclidean geometry*. MAA, 2010, vol. 37.
- [21] A. J. Fleming and A. G. Wills, "Optimal periodic trajectories for band-limited systems," *IEEE Transactions on Control Systems Technology*, vol. 17, no. 3, pp. 552–562, 2009.
- [22] R. Munnig Schmidt, G. Schitter, A. Rankers, and J. van Eijk, *The Design of High Performance Mechatronics 2nd Revised Edition*. Delft: IOS Press, 2014.
- [23] K. Johansson and C. Canudas-De-Wit, "Revisiting the lugre friction model," *IEEE Control Systems Magazine*, vol. 28, no. 6, pp. 101–114, 2008.
- [24] S. Ito, M. Poik, E. K. Csencsics, J. Schlarp, and G. Schitter, "Scanning chromatic confocal sensor for fast 3d surface characterization," in *Proceedings of the ASPE and EUSPEN Summer Topical Meeting, Advancing Precision in Additive Manufacturing*, 2018, pp. 226–231.
- [25] E. Csencsics and G. Schitter, "Parametric pid controller tuning for a fast steering mirror," in *2017 IEEE Conference on Control Technology and Applications (CCTA)*. IEEE, 2017, pp. 1673–1678.